Intestinal toxicity of the masked mycotoxin deoxynivalenol-3-β-d-glucoside

Alix Pierron, Sabria Mimoun, Leticia S Murate, Nicolas Loiseau, Yannick Lippi, Ana-Paula Bracarense, Laurence Liaubet, Gerd Schatzmayr, Franz Berthiller, Wulf-Dieter Moll, et al.

Intestinal toxicity of the masked mycotoxin deoxynivalenol-3-β-D-glucoside

Alix Pierron[1,2,3*] and Sabria Mimoun[1,2*], Leticia S. Murate[1,2,4], Nicolas Loiseau[1,2], Yannick Lippi[1,2], Ana-Paula F.L. Bracarense[4], Laurence Liaubet[5,6,7], Gerd Schatzmayr[3], Franz Berthiller[8], Wulf-Dieter Moll[3] and Isabelle P. Oswald[1,2]

[1] INRA, UMR 1331, Toxalim, Research Center in Food Toxicology, Toulouse, France
[2] Université de Toulouse, INP, UMR 1331, Toxalim, Toulouse, France
[3] BIOMIN Research Center Technopark 1, 3430 Tulln, Austria
[4] Universidade Estadual de Londrina, Lab. Patologia Animal, CP 6001, Londrina, Brazil
[5] INRA, UMR1388 Génétique, Physiologie et Systèmes d'Elevage, F-31326 Castanet-Tolosan, France.
[6] Université de Toulouse INPT ENSAT, UMR1388 Génétique, Physiologie et Systèmes d'Elevage, F-31326 Castanet-Tolosan, France.
[7] Université de Toulouse INPT ENVT, UMR1388 Génétique, Physiologie et Systèmes d'Elevage, F-31076
[8] Christian Doppler Laboratory for Mycotoxin Metabolism and Center for Analytical Chemistry, Department for Agrobiotechnology (IFA-Tulln), University of Natural Ressources and Life Sciences, Vienna, Austria
[*] equally contributed

Address correspondence to
Dr Isabelle P. Oswald
INRA, UMR-1331, Toxalim, 180 chemin de Tournefeuille, 31027 Toulouse cedex 3, France
Phone +33 582066366 E-Mail: Isabelle.Oswald@toulouse.inra.fr

Acknowledgments
The authors thank A.M. Cossalter, J. Laffitte and P. Pinton, INRA Toxalim, for sample collection and western experiments. Thanks are also due to R. Hines, BIOMIN, for language editing and to P. Pinton and I. Alassane-Kpembi for critical reading of the manuscript.
A. Pierron and L.S. Murate were supported by fellowship from CIFRE (2012/0572, jointly financed by the BIOMIN Holding GmbH, Association Nationale de la Recherche Technique and INRA) and CAPES (Brazil) respectively. The Austrian Federal Ministry of Science, Research and Economy, the Austria National Foundation for Research, Technology and Development and BIOMIN Holding GmbH are acknowledged for funding the Christian Doppler Laboratory for Mycotoxin Metabolism. The enzymatic production of D3G was performed within the Vienna Science and Technology Fund project WWTF LS12-012 by Dr. Herbert Michlmayr and Prof. Gerhard Adam.
The authors declare no conflicts of interest during the realization of the experimental work submitted.

Abstract
Natural food contaminants such as mycotoxins are an important problem for human health. Deoxynivalenol (DON) is one of the most common mycotoxin detected in cereals and grains. Its toxicological effects mainly concern the immune system and the gastrointestinal tract. This toxin is a potent ribotoxic stressor leading to MAPKinase activation and inflammatory response. DON frequently co-occurs with its glycosylated form, the masked mycotoxin deoxynivalenol-3-β-D-glucoside (D3G). The toxicity of this later compound remains unknown in mammals. This study aims to assess the ability of D3G to elicit a ribotoxic stress and to induce intestinal toxicity. The toxicity of D3G and DON (0-10µM) was studied *in vitro*, on the human intestinal Caco-2 cell line, and *ex vivo* on porcine jejunal explants. First, an *in silico* analysis revealed that D3G, contrary to DON, was unable to bind to the A site of the ribosome peptidyl transferase center, the main targets for DON toxicity. Accordingly, D3G did not activate JNK and P38 MAPKs in treated Caco-2 cells and did not alter viability and barrier function on cells, as measured by the trans epithelial electrical resistance. Treatment of intestinal explants for 4 hours with 10µM DON, induced morphological lesions and upregulated the expression of proinflammatory cytokines as measured by qPCR and pan-genomic microarray analysis. By contrast, expression profile of D3G-treated explants was similar to that of controls and these explants didn't show histomorphology alteration. In conclusion, our data demonstrated that glycosylation of DON suppress its ability to bind to the ribosome and decreases its intestinal toxicity.

Keywords: glucosylation, trichothecenes, modified mycotoxins, gut, *Fusarium,* wheat

Introduction

Mycotoxin contamination is a worldwide problem. Mycotoxins are toxic secondary metabolites produced by various molds, such as *Aspergillus, Penicillium or Fusarium* (Bennett and Klich 2003). Crops, at all stages of the food chain, are frequently contaminated by these fungi, and so by mycotoxins. Worldwide surveys indicate that 72% of all agricultural commodities are contaminated with mycotoxins (Streit et al. 2013).

Among mycotoxins, deoxynivalenol (DON) produced by *Fusarium* spp., is commonly detected in cereals and grains, particularly in wheat, barley, maize and their by-products. It is one of the most prevalent mycotoxins in food and feed (EFSA 2013). The toxicity of DON on mammals is well documented. Acute exposure induces abdominal pain, anemia, diarrhea, vomiting, circulatory shock that can result in death (Pestka 2010, Rocha et al. 2005). At chronic low doses, DON induces anorexia, growth retardation, causes neuroendocrine changes and immune modulation (Pestka and Smolinski 2005). Molecular mechanisms of action of DON are well understood. DON binds to the A-site of the peptidyl transferase center of the 60S subunit of ribosomes in eukaryotic cells and interferes with protein translation (Garreau de Loubresse et al. 2014, Pestka 2010). A ribotoxic stress response is then induced and results in the activation of mitogen-activated protein kinases (MAPK). These signaling pathways are involved in regulation of multiple biological processes including development, apoptosis, and immunity (Joshi and Platanias 2012). Upon DON exposure, MAPK activation mediates apoptosis and aberrant up-regulation of pro-inflammatory cytokines and chemokines (Pestka 2010, Wu et al. 2014a).

Upon ingestion of contaminated food, the gastrointestinal tract is particularly impacted by DON. This toxin alters the intestinal histomorphology, barrier function and nutrient absorption (Ghareeb et al. 2015, Maresca 2013, Pinton et al 2012). DON alters the integrity of the intestine resulting in a loss of mucosal integrity and a translocation of commensal and pathogenic bacteria across the epithelium (Maresca 2013, Pinton and Oswald 2014). DON also disturbs the intestinal immune responses: the toxin induces the local production of pro-inflammatory cytokines and potentiates existing intestinal inflammatory processes (Cano et al. 2013, Van De Walle et al. 2010, Vandenbroucke et al. 2011).

Associated to DON, DON-3-β-D-glucoside (D3G) is a "masked" mycotoxin produced from the enzymatic conjugation of glucose to DON in the plant (Berthiller et al. 2005, Poppenberger et al. 2003). The glucosylation reaction of DON is considered as an important detoxification mechanism occurring in plants to protect against *Fusarium*-related diseases (Lemmens et al. 2005). Thanks to the improvement of detection methods for mycotoxins, many publications investigated D3G contamination in recent years (Berthiller et al. 2013). D3G was found in cereals and cereal products all over the world at concentrations that can reach nearly half that of DON (Berthiller et al. 2009, De Boevre et al. 2012, Malachova et al. 2011).

Despite its frequent occurrence, the toxicity of D3G remains largely unknown. To date, only one group investigated the toxicity of D3G in mammals (Wu et al. 2014a). The authors observed that D3G was ineffective in evoking splenic cytokine or chemokine mRNA responses. Because D3G is poorly absorbed, the intestine can be a target for this toxin (De Nijs et al. 2012, Nagl et al. 2012, Nagl et al. 2014).

The purpose of this study was to investigate the toxicity of D3G on the intestine. An *in silico* analysis indicates that D3G is unable to bind to the ribosome and suggests a lack of toxicity of this compound. The toxicity of D3G was further assessed on intestinal cells and explants; physiological, morphological and transcriptomic analysis confirmed the absence of adverse effects of D3G. Our paper provides the first insight into the toxicity of this plant conjugate on the small intestine.

Material and methods (Additional data are available in Online resource (Online resource 1))

Toxins

Purified DON was purchased from Sigma-Aldrich (St Louis, MO, USA). D3G was isolated from DON-treated wheat (Berthiller et al. 2005) or enzymatically produced from DON (Michlmayr et al., in preparation).

Mycotoxins were dissolved in dimethyl sulfoxide (DMSO) (Sigma-Aldrich) and stored at -20°C until use.

Caco-2 cell culture and analysis

Caco-2 cells were maintained in Dulbecco's Modified Eagle Medium enriched with glutamine (Gibco, Cergy-Pontoise, France) supplemented with 10% of heat inactivated fetal bovine serum, 1% non essential amino acids (Sigma-Aldrich) and 0.5% gentamycin (Eurobio, Courtaboeuf, France). Caco-2 cells were spontaneously differentiated from confluent monolayer after 21 days of culture with medium changed every 2 days (Sambuy et al. 2005; Pinton et al 2012).

Cell viability was assessed on proliferating or differentiated cells seeded 96-well microtiter plates using the CellTiter-Glo Luminescent Cell Viability Assay (Promega, Madison, USA) according to manufacturer's instructions. Trans-epithelial electrical resistance (TEER) was measured on differentiated cells with a Millicell-ERS Voltohmmeter (Millipore, Saint-Quentin-en-Yvelines, France) as already described (Pinton et al. 2012). Expression of non-phosphorylated and phosphorylated MAPK P38 and JNK was assessed on differentiated cells by immunoblotting (Meissonnier et al 2008) using specific rabbit antibodies (Pinton et al. 2012). The expression of the proteins was estimated after normalization to GAPDH.

Intestinal jejunal explants, preparation and analysis

Jejunal explants were obtained from 5-week old crossbred castrated male piglets as described previously (Kolf-Clauw et al. 2009). They were treated for 4 hours with toxins (DON or D3G) or diluent (DMSO) and fixed in 10% formalin for histological analysis or stored at -80°C for RNA extraction.

For histological analysis, explants were embedded in paraffin wax; sections (5 µm) were stained with hematoxylin and eosin for histopathological evaluation (Bracarense et al. 2012).

For gene expression analysis, total RNA was extracted in lysing matrix D tubes (MP Biomedicals, Illkirch, France) containing guanidine thiocyanate-acid phenol (Eurobio). Quality of these samples was assessed (Agilent RNA 6000 Nano Kit Quick, Agilent Bioanalyzer 2100); the mean RNA Integrity Number (RIN) of these mRNA was 6.32 ± 0.83.

Reverse transcription and RT-qPCR steps were performed as already described (Halloy et al. 2005; Gourbeyre et al. 2015). Primers are indicated in the Table (Online ressource 2). Amplification efficiency and initial fluorescence were determined by the ΔCt method. Obtained values were normalized using two reference genes, ribosomal protein L32 (RPL32) and cyclophillin A. mRNA expression levels were expressed relative to the mean of the control.

The 60K microarray (Voillet et al. 2014) was used as described in the supplemental Material (see Supplemental Material, Part Methods). The experimental details are available in the Gene Expression Omnibus (GEO) database under accession GSE66918 (http://www.ncbi.nlm.nih.gov/geo/query/acc.cgi?token=olixoosedvmdnqr&acc=GSE66918). Microarray data from Feature Extraction software was analyzed with R using Bioconductor packages.

Statistical Analysis

The Fisher test on equality of variances, one-way ANOVA and Bonferroni as test post-hoc were used to compare the effect of DON and D3G on Caco-2 cells and explants; p values < 0.05 were considered significant.

For microarray data, statistical analysis was performed with R 3.0.1 software.

Results

In silico analysis of the interaction of DON and D3G with ribosome

A recent paper shows that DON binds to the 60S subunit inside the A-site of the peptidyl transfer center of yeast ribosome (Garreau de Loubresse et al. 2014). The crystallographic data (4UJX) were used to compare the ability of DON and D3G to interact with the ribosome (Figure 1, Online resources 3 and 4). DON is able to fit in the pocket of the A-site of the ribosome 60S subunit. In this position, the 3-hydroxyl group of DON is associated with a magnesium atom and stabilized by other nucleotides. The alignment of the common backbone of D3G and DON allows us to generate a model of interaction with the ribosome and to study the sterical hindrance of glucoside inside the A-site pocket. Even in the absence of the magnesium atom, the size of the pocket is too small for the glucosyl group, showing that D3G cannot sterically bind the ribosome 60S subunit A-site pocket.

Inability of D3G to activate MAPK

As other ribosome-binding translational inhibitors, DON rapidly activates MAPK. As expected (Pinton et al. 2012), 1 hour of exposure of differentiated Caco-2 monolayers to10 µM DON, significantly increased the expression of phosphorylated p38 and phosphorylated JNK but did not changed the expression of the non phosphorylated MAPK. By contrast the activation of these MAPK upon treatment with D3G was similar to untreated control monolayers (Figure 2A). Taken together our data indicate that D3G does not bind to ribosome and does not activate MAPK. The lack of MAPK activation is indicative of an absence of toxicity of D3G and was further tested.

D3G does not impair cell viability and barrier function of human intestinal cells

Comparative toxicity of DON and D3G was evaluated both on proliferating (Figure 3) and differentiated (Figure 2B and C) Caco-2 human cells. After 48 hours of exposure to DON the viability of the proliferating cells was decreased in a dose dependent-manner, and 50% inhibition was observed at 1.30 µM DON. Exposure to 10 µM DON for 48 hours reduced cell viability by approximately 80%. By contrast, no cytotoxicity was observed on Caco-2 cells treated with 0-10 µM D3G (Figure 3) or higher concentrations (up to 100 µM, data not shown).

The comparative toxicity of D3G and DON was also performed on differentiated Caco-2 cells. As already described (Bony et al 2006, Vandenbroucke et al 2011) differentiated cells are fairly resistant to DON and toxin concentration of 30µM or higher are needed to induce a significant decrease of viability (Figure 2C). At 10µM, a non-cytotoxic concentration, DON induced a significant decrease of TEER (Figure 2B). The decrease was time-dependent and the cell viability reached 69%, 42%, 30% and 19% after 2, 4, 6 and 8 days of exposure to DON respectively. By contrast cell treatment with D3G did not decrease TEER.

D3G does not induce histological and functional alterations in intestinal explants

In order not to restrict the observations to an intestinal cell line, the comparative toxicity of DON and D3G was also performed on whole intestinal tissue, using porcine jejunal explants.

Control intestinal explants displayed normal villi lined with columnar enterocytes and goblet cells (Figure 4A). As already described (Pinton et al. 2012), the main histological changes observed on explants after 4 hours incubation with 10 µM DON were multifocal to diffuse villi atrophy, multifocal villi fusion, necrosis of apical enterocytes and cellular debris (Figure 4B). Conversely, explants exposed to D3G showed normal villi height lined with columnar enterocytes. However mild cellular debris in the apical surface and lymphatic vessel dilation were also observed in D3G treated explants (Figure 4C).

D3G by contrast to DON does not alter gene expression profile in intestinal explants

To complete the investigations on the intestinal toxicity, gene expression was analyzed by RT-qPCR and microarray.

Exposure to 10 µM DON for 4 hours significantly increased the expression of IL-1α, TNFα, IL-1β, IL-8, IL-17A and IL-22 (3.5 to 17.4-fold increase, Figure 3B). By contrast, no increase expression of these pro-inflammatory cytokines was observed in D3G treated explants, demonstrating that this toxin was not able to induce an intestinal inflammation.

To deeper investigate the extent of DON and D3G on gene expression, a 60K microarray covering the whole transcriptome was used (Voillet et al. 2014). Principal component analysis, Venn diagram and heat map indicate a similar expression pattern of D3G-treated and control explants (Figure 5). In contrast, two clusters were distinguished in DON treated samples: cluster 1 contains 303 genes (corresponding to 681 probes) that are up-regulated by the mycotoxin, cluster 2 includes 33 down-regulated genes (corresponding to 66 probes). As expected, the 6 pro-inflammatory cytokines tested in RT-qPCR were also up-regulated in the gene expression microarray analysis and a linear regression revealed a strong correlation between these two techniques (R^2=0.96). Besides pro-inflammatory cytokines, DON treatment also up-regulates (fold change > 2.4) genes involved in inflammation and immune response such as *CCL20, CXCL2, PRDM1, AREG, CSF2, FOSL1* as well as genes involved in oxidative stress, NFkB activation pathway, cell cycle regulation and apotosis. Down regulated genes concerned molecular transport (*ABCC2, SLC15A1,* and *SLC9A2*) and mitochondrial functions (*CPT1A*).

Discussion

Food safety authorities such as JECFA (WHO-FAO) and EFSA recognized the need for regulating masked mycotoxins. However, scientific data especially concerning the toxicity of these toxins are scarce (JECFA 2011). The aim of our work was to assess the toxicological relevance of D3G on intestinal gut health in comparison to the parent molecule DON. The intestine is the first line of defense protecting against harmful luminal food contaminants. It acts as physical barrier limiting penetration of agents and releases chemical and immunological mediators that contribute to the development of innate immune responses and maintenance of intestinal homeostasis (Pinton and Oswald 2014, Maresca 2013).

DON induces several pathophysiological effects in experimental animals and in cells culture that are attributable, in part, to ribotoxic stress and the activation of MAPK (Pestka 2010, Pinton and Oswald 2014). *In silico* analysis demonstrates that glucoside-residue of D3G hinders interaction of this masked mycotoxin with the ribosome. This result suggests an absence of ribotoxic stress and literature data report a reduced inhibitory activity of D3G on wheat ribosomes (Poppenberger et al. 2003). We further observed that D3G, in contrast to DON did not induce phosphorylation of JNK and P38 proteins in Caco-2 cells. These results suggest an absence of toxic effect of D3G on mammalian cells as recently described for microbial cells (Suzuki and Iwahashi 2015). This hypothesis was further tested and the impact of DON and D3G was compared on the Caco-2 intestinal cell lines and intestinal explants. Mycotoxins were tested at 10 µM, a concentration corresponding to food contaminated at 3mg/kg (Sergent et al. 2006). We confirmed that DON induced cytotoxicity and alter intestinal barrier integrity in human intestinal epithelial cells (Alassane-Kpembi et al. 2013, Sergent et al. 2006). In contrast, D3G was not cytotoxic on intestinal cells and did not impaired transepithelial electrical resistance.

The impact of DON and D3G was further assessed on porcine jejunum tissue. Pig can be regarded as a good model of extrapolation to humans (Helke and Swindle 2013). DON induces morphological injury (Osselaere et al. 2013) and inflammation on porcine jejunum explants (Cano et al. 2013). Cytokines and chemokines are sensitive biomarkers for DON exposure (Pestka 2010, Wu et al. 2014a). Indeed, proinflammatory response upon DON exposure has been described both *in vitro* in cell lines from murine, human and porcine origins as well as *in vivo* in several organs (Cano et al. 2013, Pestka 2010). In contrast to DON, D3G did not induced any histological damage and was largely incapable of evoking ribotoxin-induced cytokine production on pig jejunum confirming data obtained *in vivo* in mouse spleens (Wu et al. 2014a). The lack of induction of gene expression by D3G was further demonstrated using a pan-genomic DNA array containing 62,976 probes. Indeed the transcriptomic analysis revealed that no probes were differentially expressed between control explants and the

one treated with D3G.

As already mentioned data concerning metabolism and toxicity of D3G are very scarce. Only one study has been performed in mice that indicated that D3G was ineffective in evoking inducing the expression of cytokine or chemokine mRNA in the spleen (Wu et al. 2014a). To the best of our knowledge, our experiment provides the first data on the lack of toxic effect of D3G on human cells and on the intestine. It has been described that D3G are considerably less bioavailable in mammals when compared to DON. Indeed, following oral administration, only small percentage of applied dose of D3G was found in urine in rats and piglets (Nagl et al. 2012, Nagl et al. 2014). Moreover, in a human volunteer consuming a diet naturally contaminated with D3G, the masked mycotoxin could not be detected in urine (Warth et al. 2013). Interestingly, De Nijs et al. (2012) observed that D3G is less absorbed by human intestinal Caco-2 cells than DON. In fact, because of its higher molecular weight and its increased polarity, D3G would have a reduced ability to enter the cells by lipid diffusion or through membrane transporters if such transporters are involved.

In vitro data indicated that D3G can be cleaved to DON by lactic acid bacteria and human feces (Berthiller et al. 2011, Dall'Erta et al. 2013, Gratz et al. 2013). These findings correlate well with those of Nagl et al. (2012, 2014) underlining that the majority of oral administrated D3G was recovered as DON in feces. *In vivo* the conversion of D3G to its toxic aglycone may occur in the distal part of the gut, while ingested DON is absorbed in the proximal part of the small intestine (Maresca 2013). Hence, ingestion of D3G contaminated food might lead to a release of DON in the distal part of intestine, shifting the toxic effect of D3G in the distal part of the intestine as already described for ingestion of DON-contaminated food in the presence of this adsorbing agent (Osselaere et al. 2013). Nevertheless acute ingestion of high doses of D3G does not induce inflammatory reaction in mice and mink (Wu et al. 2014a) nor emetic effect in mink (Wu et al. 2014b). Of note D3G causes an anorectic response in mice suggesting that this later effect is mediated through a different mechanism than ribotoxic stress involving CCK and PYY release from enteroendocrine cells via GPCRs and TRP Channels (Zhou and Pestka 2015).

As demonstrated in this study exploring intestinal explants by microarray analysis offers a promising approach for assessing the intestinal toxicity of mycotoxins. Using intestinal explants allows integrating the overall complexity of the gastrointestinal tract including their cytoarchitectures, intercellular interactions and the presence of target cells. The microarray analysis allows having a view of the modulated genes. Using this approach we demonstrated the lack of effect of D3G while confirming the interference of DON with the immune response. Effects of DON using microarray analysis have previously been described *in vitro* in human T-lymphocyte cell line (Jurkat cells) and human peripheral blood mononuclear cells (PBMCs) or *in vivo* in murine thymus, exposed to DON (Katika et al. 2012, van Kol et al. 2011). We also observe the interference of DON with genes involved in other biological functions such as oxidative stress, cell cycle molecular transport and mitochondrial functions. As recently described *in vivo* (Alizadeh et al. 2015), a decreased expression of mRNA levels of efflux transporters was observed also in intestinal explants exposed to DON. Studies reported that DON is a substrate for ABC transporter (Videmann et al, 2007) thus a decrease expression of efflux protein would decrease uptake of DON by intestinal cells and thereby decrease its toxicity.

The approach combining explant and microarray can be used to investigate the effect of other contaminants or additives on the intestine and may represent an interesting tool for health risk assessment.

This study significantly extends the current knowledge about intestinal toxicity of D3G. D3G is not toxic by itself but may pose a risk for gut health through its reconversion into its parent mycotoxin DON.

References

Alassane-Kpembi I, Kolf-Clauw M, Gauthier T, Abrami R, Abiola FA, Oswald IP and Puel O (2013) New insights into mycotoxin mixtures: The toxicity of low doses of Type B trichothecenes on intestinal epithelial cells is synergistic. Toxicol Appl Pharmacol. 272:191-198 doi:10.1016/j.taap.2013.05.023

Alizadeh A, Braber S, Akbari P, Garssen J and Fink-Gremmels J (2015) Deoxynivalenol Impairs Weight Gain and Affects Markers of Gut Health after Low-Dose, Short-Term Exposure of Growing Pigs. Toxins (Basel). 7:2071-95. doi:10.3390/toxins7062071.

Bennett JW and Klich M (2003) Mycotoxins. Clin Microbiol Rev. 16:497-516. doi: 10.1128/CMR.16.3.497-516.2003

Berthiller F, Crews C, Dall'Asta C, Saeger SD, Haesaert G, Karlovsky P, Oswald IP, Seefelder W et al. (2013) Masked mycotoxins: a review. Mol Nutr Food Res 57:165-186 doi:10.1002/mnfr.201100764

Berthiller F, Dall'Asta C, Corradini R, Marchelli R, Sulyok M, Krska R, Adam G and Schuhmacher R (2009) Occurrence of deoxynivalenol and its 3-beta-D-glucoside in wheat and maize. Food Addit Contam Part A Chem Anal Control Expo Risk Assess. 26:507-511 doi:10.1080/02652030802555668

Berthiller F, Dall'Asta C, Schuhmacher R, Lemmens M, Adam G and Krska R (2005) Masked mycotoxins: determination of a deoxynivalenol glucoside in artificially and naturally contaminated wheat by liquid chromatography-tandem mass spectrometry. J Agric Food Chem. 53:3421-3425 doi:10.1021/jf047798g

Berthiller F, Krska R, Domig KJ, Kneifel W, Juge N, Schuhmacher R and Adam G (2011) Hydrolytic fate of deoxynivalenol-3-glucoside during digestion. Toxicol Lett. 206:264-267 doi:10.1016/j.toxlet.2011.08.006

Bony S, Carcelen M, Olivier L and Devaux A (2006) Genotoxicity assessment of deoxynivalenol in the Caco-2 cell line model using the Comet assay. Toxicol Lett 166(1): 67-76 doi:10.1016/j.toxlet.2006.04.010

Bracarense AP, Lucioli J, Grenier B, Drociunas Pacheco G, Moll WD, Schatzmayr G and Oswald IP (2012) Chronic ingestion of deoxynivalenol and fumonisin, alone or in interaction, induces morphological and immunological changes in the intestine of piglets. Br J Nutr. 107:1776-1786 doi:10.1017/S0007114511004946

Cano PM, Seeboth J, Meurens F, Cognie J, Abrami R, Oswald IP and Guzylack-Piriou L (2013) Deoxynivalenol as a new factor in the persistence of intestinal inflammatory diseases: an emerging hypothesis through possible modulation of Th17-mediated response. PLoS One. 8:e53647. doi:10.1371/journal.pone.0053647

Dall'Erta A, Cirlini M, Dall'Asta M, Del Rio D, Galaverna G and Dall'Asta C (2013) Masked mycotoxins are efficiently hydrolyzed by human colonic microbiota releasing their aglycones. Chem Res Toxicol. 26:305-312 doi:10.1021/tx300438c

De Boevre M, Di Mavungu JD, Maene P, Audenaert K, Deforce D, Haesaert G, Esckhout M, Callebaut A et al. (2012) Development and validation of an LC-MS/MS method for the simultaneous determination of deoxynivalenol, zearalenone, T-2-toxin and some masked metabolites in different cereals and cereal-derived food. Food Addit Contam Part A. 29:819-835 doi:10.1080/19440049.2012.656707

De Nijs M, Van den Top HJ, Portier L, Oegema G, Kramer E, Van Egmond HP and Hoogenboom RLAP (2012) Digestibility and absorption of deoxynivalenol-3-β-glucoside in in vitro models. World Mycotoxin J. 5:319-324 doi:10.1080/19440049.2013.820846.

EFSA (2013) Deoxynivalenol in food and feed: occurrence and exposure. EFSA J. 11:3379. doi:10.2903/j.efsa.2013.3379

Garreau de Loubresse N, Prokhorova I, Holtkamp W, Rodnina MV, Yusupova G and Yusupov M (2014) Structural basis for the inhibition of the eukaryotic ribosome. Nature. 513:517-522. doi:nature13737

Ghareeb K, Awad WA, Bohm J and Zebeli Q (2015) Impacts of the feed contaminant deoxynivalenol on the intestine of monogastric animals: poultry and swine. J Appl Toxicol. 35:327-337. doi:10.1002/jat.3083

Gratz SW, Duncan G and Richardson AJ (2013) The human fecal microbiota metabolizes deoxynivalenol and deoxynivalenol-3-glucoside and may be responsible for urinary deepoxy-deoxynivalenol. Appl Environ Microbiol. 79:1821-1825. doi:10.1128/AEM.02987-12

Halloy DJ, Gustin PG, Bouhet S and Oswald IP (2005) Oral exposure to culture material extract containing fumonisins predisposes swine to the development of pneumonitis caused by *Pasteurella multocida*. Toxicology. 213:34-44. doi:10.1151/vetres:2004012

Helke KL and Swindle MM (2013) Animal models of toxicology testing: the role of pigs. Expert Opin Drug Metab Toxicol. 9:127-139. doi:10.1517/17425255.2013.739607

JECFA (2011) Evaluation of certain contaminants in food: seventy-second report of the Joint FAO/WHO Expert Committee on Food Additives. WHO technical report series; no 959

Joshi S and Platanias LC (2012) Mnk Kinases in Cytokine Signaling and Regulation of Cytokine Responses. Biomol Concepts. 3:127-139. doi:10.1515/bmc-2011-0057

Katika MR, Hendriksen PJ, Shao J, van Loveren H and Peijnenburg A (2012) Transcriptome analysis of the human T lymphocyte cell line Jurkat and human peripheral blood mononuclear cells exposed to deoxynivalenol (DON): New mechanistic insights. Toxicol Appl Pharmacol. 264:51-64. doi:10.1016/j.taap.2012.07.017

Kolf-Clauw M, Castellote J, Joly B, Bourges-Abella N, Raymond-Letron I, Pinton P and Oswald IP (2009) Development of a pig jejunal explant culture for studying the gastrointestinal toxicity of the mycotoxin deoxynivalenol: Histopathological analysis. Toxicol in Vitro. 23:1580-1584. doi:10.1016/j.tiv.2009.07.015

Lemmens M, Scholz U, Berthiller F, Dall'Asta C, Koutnik A, Schumacher R, Adam G, Buerstmayr H et al. (2005) The ability to detoxify the mycotoxin deoxynivalenol colocalizes with a major quantitative trait locus for *Fusarium* head blight resistance in wheat. Mol Plant Microbe Interact. 18:1318-1324. doi:10.1094/MPMI-18-1318

Malachova A, Dzuman Z, Veprikova Z, Vaclavikova M, Zachariasova M and Hajslova J (2011) Deoxynivalenol, deoxynivalenol-3-glucoside, and enniatins: the major mycotoxins found in cereal-based products on the Czech market. J Agric Food Chem. 59:12990-12997. doi:10.1021/jf203391x

Maresca M (2013) From the gut to the brain: journey and pathophysiological effects of the food-associated mycotoxin Deoxynivalenol. Toxins 5:784-820 doi:10.3390/toxins5040784

Meissonnier GM, Laffitte J, Raymond I, Benoit E, Cossalter AM, Pinton P, Bertin G, Oswald IP and Galtier P (2008) Subclinical doses of T-2 toxin impair acquired immune response and liver cytochrome P450 in pigs. Toxicology. 247:46-54. doi: 10.1016/j.tox.2008.02.003.

Nagl V, Schwartz H, Krska R, Moll WD, Knasmüller S, Ritzmann M, Adam G and Berthiller F. (2012) Metabolism of the masked mycotoxin deoxynivalenol-3-glucoside in rats. Toxicol Lett. 213:367-373 doi:10.1016/j.toxlet.2012.07.024

Nagl V, Woechtl B, Schwartz-Zimmermann HE, Hennig-Pauka I, Moll WD, Adam G and Berthiller F (2014) Metabolism of the masked mycotoxin deoxynivalenol-3-glucoside in pigs. Toxicol Lett. 229:190-197 doi: 10.1016/j.toxlet.2014.06.032

Osselaere A, Santos R, Hautekiet V, De Backer P, Chiers K, Ducatelle R and Croubels S (2013) Deoxynivalenol impairs hepatic and intestinal gene expression of selected oxidative stress, tight junction and inflammation proteins in broiler chickens, but addition of an adsorbing agent shifts the effects to the distal parts of the small intestine. PLoS One. 8:e69014 doi:10.1371/journal.pone.0069014 PONE-D-13-06016

Pestka JJ (2010) Deoxynivalenol: mechanisms of action, human exposure, and toxicological relevance. Arch Toxicol. 84:663-679 doi:10.1007/s00204-010-0579-8

Pestka JJ and Smolinski AT (2005) Deoxynivalenol: toxicology and potential effects on humans. J Toxicol Environ Health B Crit Rev. 8:39-69 doi:10.1080/10937400590889458

Pinton P and Oswald IP (2014) Effect of deoxynivalenol and other Type B trichothecenes on the intestine: a review. Toxins (Basel). 6:1615-1643 doi:10.3390/toxins6051615

Pinton P, Tsybulskyy D, Lucioli J, Laffitte J, Callu P, Lyazhri F, Grosjean F, Bracarense AP et al. (2012) Toxicity of deoxynivalenol and its acetylated derivatives on the intestine: differential effects on morphology, barrier function, tight junction proteins, and mitogen-activated protein kinases. Toxicol Sci. 130:180-190 doi: 10.1093/toxsci/kfs239

Poppenberger B, Berthiller F, Lucyshyn D, Sieberer T, Schuhmacher R, krska R, Kuchler K, Glossl J et al. (2003) Detoxification of the Fusarium mycotoxin deoxynivalenol by a UDP-glucosyltransferase from Arabidopsis thaliana. J Biol Chem. 278:47905-47914. doi:10.1074/jbc.M307552200

Rocha O, Ansari K and Doohan FM (2005) Effects of trichothecene mycotoxins on eukaryotic cells: a review Food Addit Contam. 22:369-378. DOI: 10.1080/02652030500058403

Sambuy Y, De Angelis I, Ranaldi G, Scarino ML, Stammati A and Zucco F (2005) The Caco-2 cell line as a model of the intestinal barrier: influence of cell and culture-related factors on Caco-2 cell functional characteristics. Cell Biol Toxicol. 21:1-26 doi:10.1007/s10565-005-0085-6

Sergent T, Parys M, Garsou S, Pussemier L, Schneider YJ and Larondelle Y (2006) Deoxynivalenol transport across human intestinal Caco-2 cells and its effects on cellular metabolism at realistic intestinal concentrations. Toxicol Lett. 164:167-176. doi:10.1016/j.toxlet.2005.12.006

Streit E, Naehrer K, Rodrigues I and Schatzmayr G (2013) Mycotoxin occurrence in feed and feed raw materials worldwide: long-term analysis with special focus on Europe and Asia. J Sci Food Agric. 93:2892-2899. doi:10.1002/jsfa.6225

Suzuki T and Iwahashi Y (2015) Low toxicity of deoxynivalenol-3-glucoside in microbial cells. Toxins (Basel). 7:187-200. doi:10.3390/toxins7010187

Van De Walle J, During A, Piront N, Toussaint O, Schneider YJ and Larondelle Y (2010) Physio-pathological parameters affect the activation of inflammatory pathways by deoxynivalenol in Caco-2 cells. Toxicol In Vitro. 24:1890-1898. doi:10.1016/j.tiv.2010.07.008

van Kol SW, Hendriksen PJ, van Loveren H and Peijnenburg A (2011) The effects of deoxynivalenol on gene expression in the murine thymus. Toxicol Appl Pharmacol. 250:299-311. doi:10.1016/j.taap.2010.11.001

Vandenbroucke V, Croubels S, Martel A, Verbrugghe E, Goossens J, Van Deun K, Boyen F, Thompson A et al. (2011) The mycotoxin deoxynivalenol potentiates intestinal inflammation by *Salmonella* typhimurium in porcine ileal loops. PLoS One. 6:e23871. doi:10.1371/journal.pone.0023871

Videmann B, Tep J, Cavret S and Lecoeur S (2007) Epithelial transport of deoxynivalenol: involvement of human P-glycoprotein (ABCB1) and multidrug resistance-associated protein 2 (ABCC2). Food Chem Toxicol. 45:1938-47. doi:10.1016/j.fct.2007.04.011

Voillet V, San Cristobal M, Lippi Y, Martin PG, Lannuccelli N, Lascor C, Vignoles F, Billon Y et al. (2014) Muscle transcriptomic investigation of late fetal development identifies candidate genes for piglet maturity. BMC Genomics. 15:797 doi:10.1186/1471-2164-15-797

Waché YJ, Hbabi-Haddioui L, Guzylack-Piriou L, Belkhelfa H, Roques C and Oswald IP. (2009) The mycotoxin deoxynivalenol inhibits the cell surface expression of activation markers in human macrophages. Toxicology. 262:239-44. doi: 10.1016/j.tox.2009.06.014

Warth B, Sulyok M, Berthiller F, Schuhmacher R and Krska R (2013) New insights into the human metabolism of the Fusarium mycotoxins deoxynivalenol and zearalenone. Toxicol Lett. 220:88-94 doi:10.1016/j.toxlet.2013.04.012

Wu W, He K, Zhou H-R, Berthiller F, Adam G, Sugita-Konishi Y, Watanabe M, Krantis A et al. (2014a) Effects of oral exposure to naturally-occurring and synthetic deoxynivalenol congeners on proinflammatory cytokine and chemokine mRNA expression in the mouse. Toxicol Appl Pharmacol. 278:107-115. doi:http://dx.doi.org/10.1016/j.taap.2014.04.016

Wu W, Zhou H-R, Bursian SJ, Pan X, Link JE, Berthiller F, Adam G, Krantis A, et al (2014b) Comparison of anorectic and emetic potencies of deoxynivalenol (Vomitoxin) to the plant metabolite deoxynivalenol-3-glucoside and synthetic deoxynivalenol derivatives EN139528 and EN139544. Toxicol Sci. 142:167–181. doi: 10.1093/toxsci/kfu166

Zhou HR and Pestka JJ (2015) Deoxynivalenol (Vomitoxin)-Induced Cholecystokinin and Glucagon-Like Peptide-1 Release in the STC-1 Enteroendocrine Cell Model is Mediated by Calcium-Sensing Receptor and Transient Receptor Potential Ankyrin-1 Channel. Toxicol Sci. 145:407-17. doi: 10.1093/toxsci/kfv061

Figures

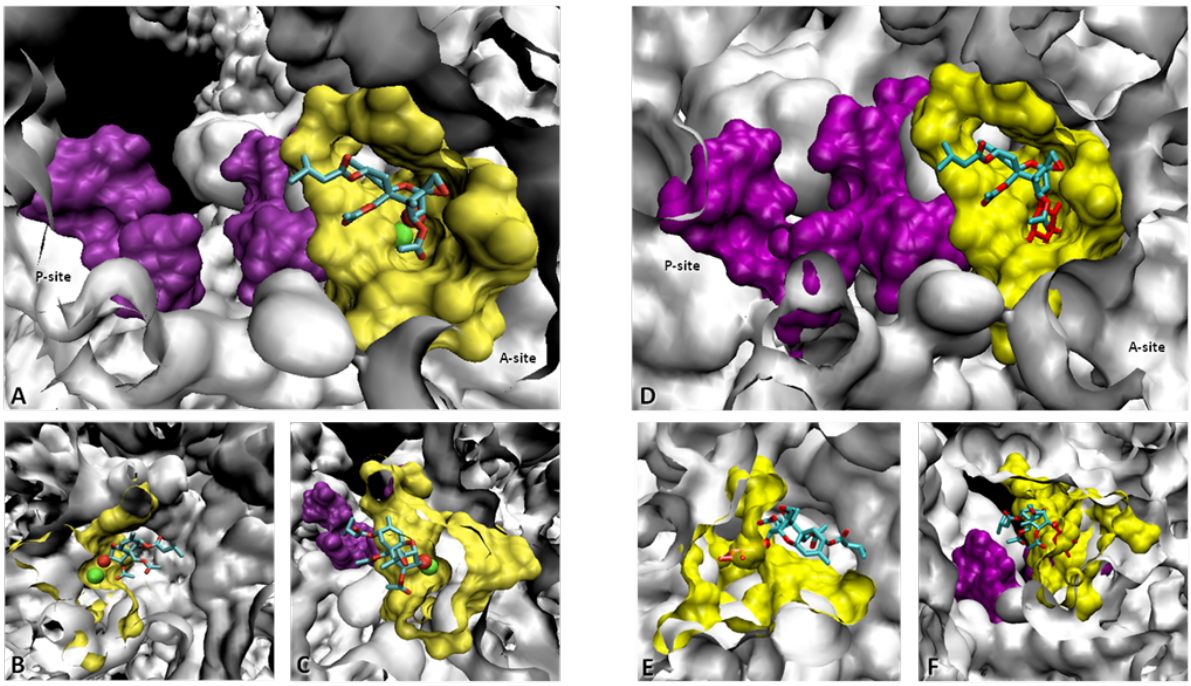

Figure 1. Interaction between the Ribosome 60S subunit binding site and DON or D3G (Front view: panels A and D, right orthogonal view: panels B and E, left orthogonal view: panels C and F. P and A sites of the yeast ribosome 60S subunit are colored in purple and yellow respectively).
Panels A, B and C: detailed views of the co-crystal (4UJX) of DON inside the A-site. The 3-hydroxyl group of DON has been pointed out being in red CPK representation. The magnesium atom inside the A-site pocket has been pointed out in green CPK representation.
Panels D, E and F: detailed of the interaction model of D3G inside the A-site after alignment of the backbone of D3G over the DON. The 3-O-glucosyl group of D3G has been colored in red. Videos showing 360°C view of DON and D3G inside the A-site of the ribosome 60S subunit are available as Supplemental Material Figures S1 and S2

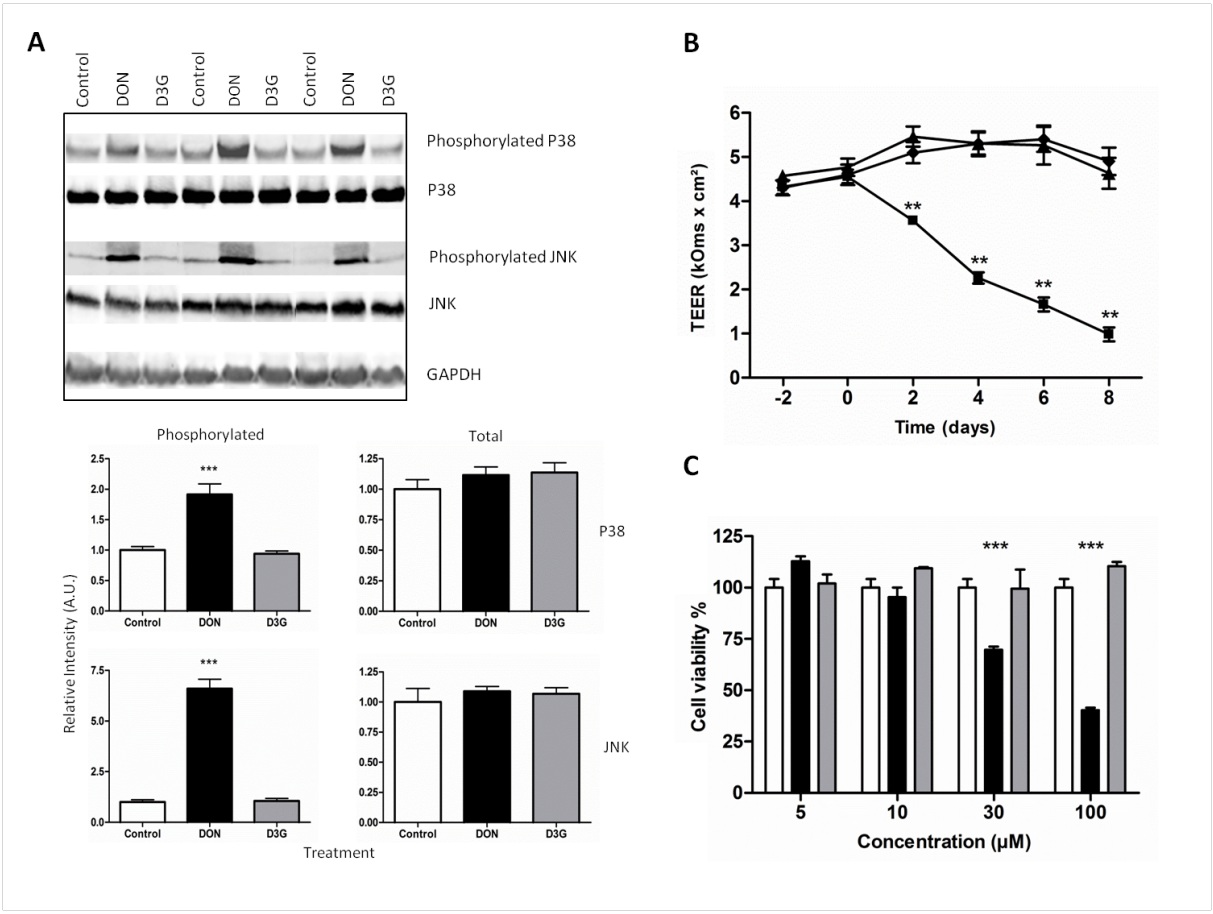

Figure 2. Effects of DON and D3G on differentiated human intestinal epithelial cells

Panel A: Effect on the activation of MAPK. Caco-2 cells, differentiated on inserts, were treated for 1h with 10 µM toxins and analyzed by western blot for expression of total and phosphorylated p38 and JNK and GAPDH as a protein loading control. Results are expressed as mean ± SEM of 3-4 independent experiments, **p<0.01, ***p<0.001.

Panel B: Effect on trans-electrical epithelial resistance. Caco-2 cells, differentiated on inserts, were treated at day 0 with 10 µM of diluent (♦), D3G (▲) or DON (■) and TEER was measured.

Panel C: Effect on cytotoxicity. Caco-2 cells, differentiated in plate, were incubated with increasing concentrations of diluent, D3G or DON for 8 days. Cell viability evaluated by measurement of ATP, is expressed as % of control cells.

Results are expressed as mean ± SEM of 3-4 independent experiments, **p<0.01, ***p<0.001.

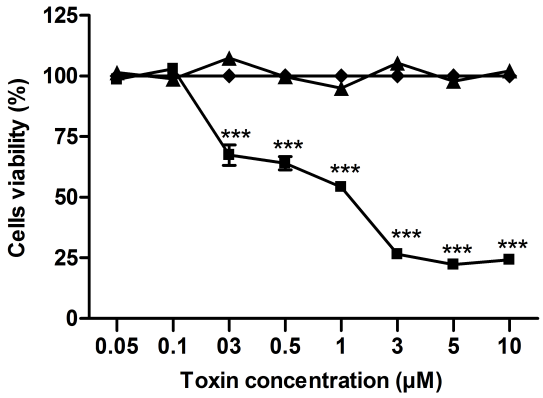

Figure 3. Toxicity of DON and D3G on proliferating human intestinal epithelial cells.
Proliferative Caco-2 cells were incubated with increasing concentrations of diluent (♦), D3G (▲) or DON (■) for 48 hours. Cell viability evaluated by measurement of ATP, is expressed as % of control cells.
Results are expressed as mean ± SEM of 3-4 independent experiments, ***p<0.001.

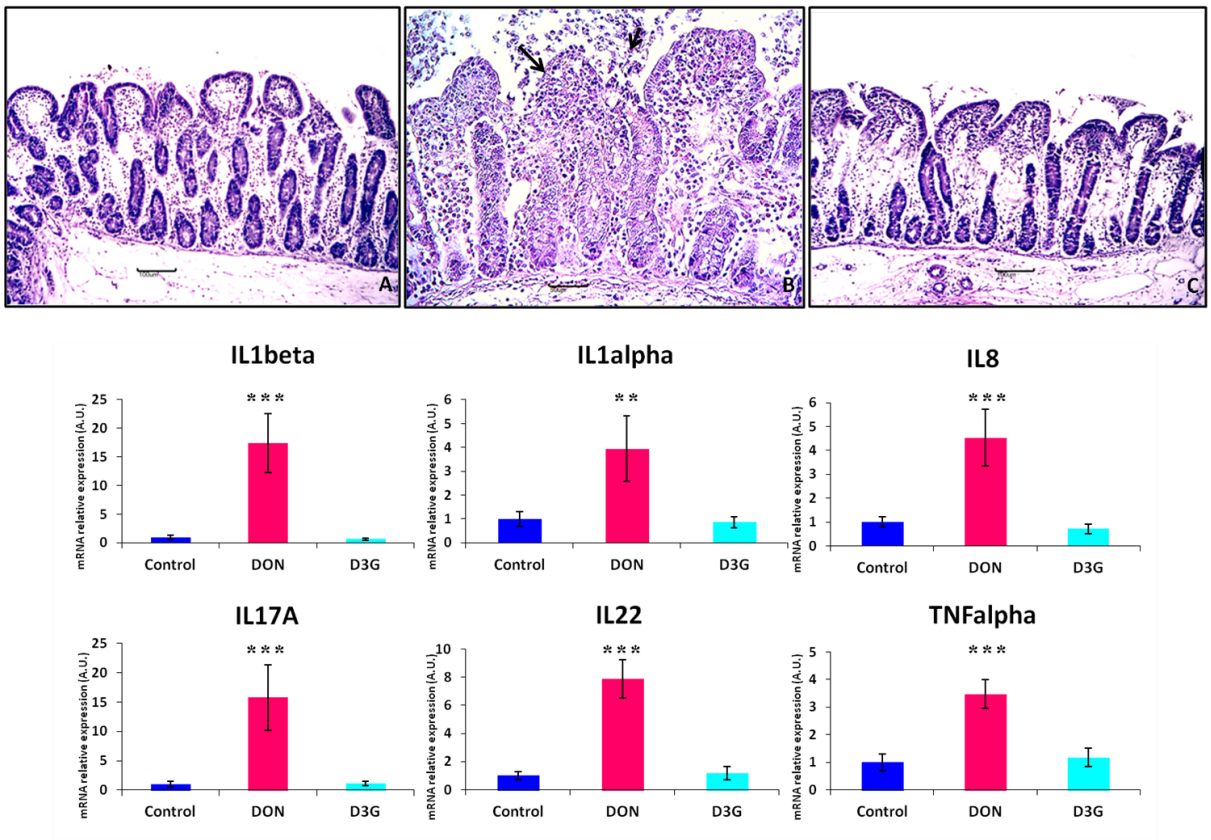

Figure 4. Effects of DON and D3G on intestinal explants:
Morphology (upper panels) and inflammation (lower panels)
Upper panels: Jejunal explants were exposed for 4hours, to diluent (3A), 10 µM DON (3B) or 10 µM D3G (3C) and stained with hematoxylin and eosin. Arrowheads indicate necrosis of apical enterocytes and cellular debris. Bar 100 µm (3A and 3B), 50 µm (3C).
Lower panels: Jejunal explants were exposed for 4hours, to diluent or 10 µM toxins and relative expression of mRNA encoding for pro-inflammatory cytokines was measured by RT-qPCR. Data are normalized to diluent and expressed, in arbitrary unit, as mean ± SEM of explants from 6 animals, **p<0.01; ***p<0.001.

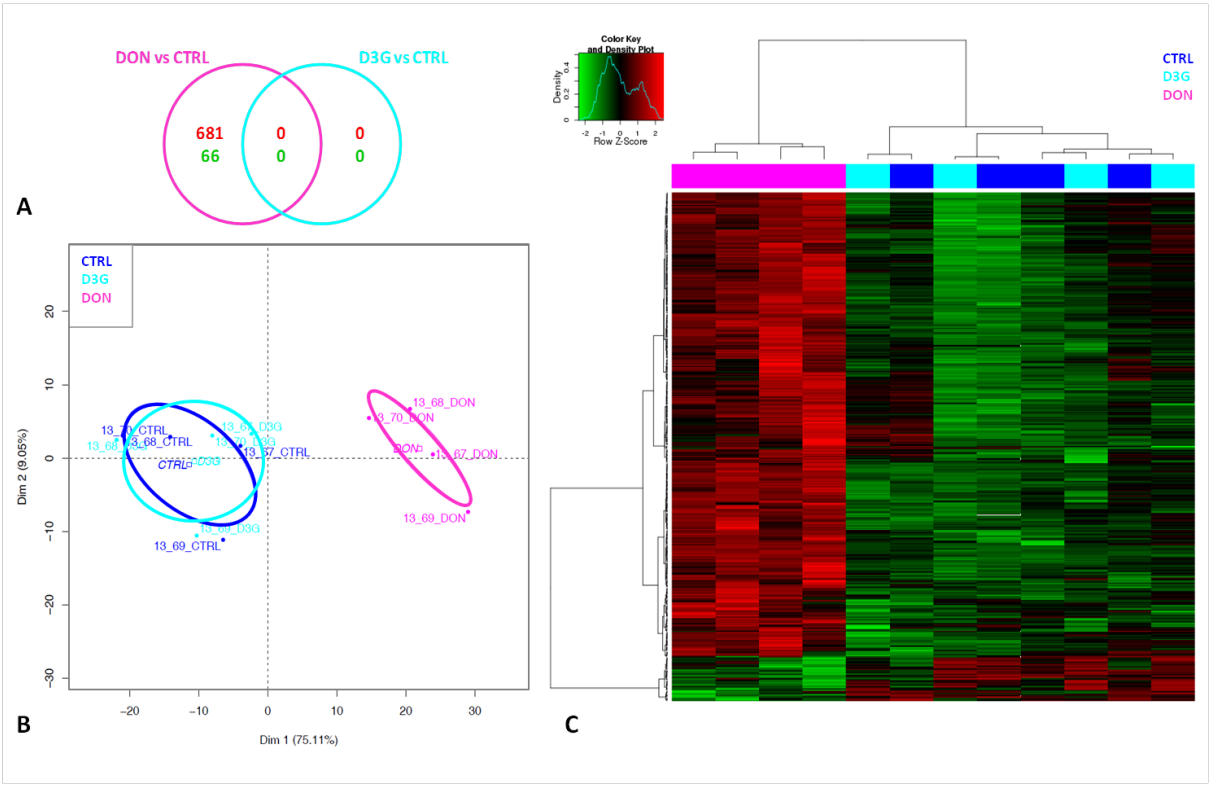

Figure 5. Gene expression profile of intestinal explants exposed to DON or D3G

Jejunal explants from 4 different animals were exposed for 4hours, to diluent or 10 µM toxins and gene expression was analyzed with a 60K microarray.

Panel A: Venn diagram illustrating the overlaps between the probes significantly up- or down-regulated in response to DON or D3G treatment.

Panel B: Principal Component Analysis of differentially expressed probes between DON/D3G and control (747 with BH adjusted p-*value* < 0.05).

Panel C: Heat map representing differentially expressed probes between DON, D3G and control explants. Red and green colors indicate values above and below the mean (average Z-score) respectively. Black color indicates values close to the mean.

ESM_ 1: Supplemental Material and methods

Caco-2 cell culture

The human epithelial colorectal adenocarcinoma cells Caco-2 (passages 99 - 106) obtained from the TC7 were used. Cells were maintained in a humidified atmosphere of 90% air and 5% CO2 at 37°C. Medium was refreshed every 2 days and cells were passaged one a week. Cells were trypsinized using Trypsin –Versene (EDTA, Eurobio) and were diluted in culture medium. Caco-2 cells were spontaneously differentiated from confluent monolayer after 21 days of culture with medium changed every 2 days (Sambuy et al. 2005; Pinton et al 2012).

Cell viability assay

Cell viability assay were performed with the CellTiter-Glo Luminescent Cell Viability (Promega, Madison, USA). Cells were seeded at the density of $1.56.10^5$cells/cm² in 96-well microtiter plates (surface area 0.28cm²) (Greiner bio-one, Vilvoorde, Belgique).

For proliferating cells, after 24 hours of incubation, cells were exposed for 48 hours at different doses of diluents (DMSO) or toxins: DON or D3G. For differentiating cells, cell viability assay was performed after 21 days of differentiation and cells were exposed for 8 days at different doses of diluents (DMSO) or toxins: DON or D3G. Luminescence was measured with a spectrophotometer (TECAN Infinite M200, Männedorf, Switzerland).

Trans-epithelial electrical resistant measurement

Cells ($1.34x10^5$cells/cm² of seeding) were grown until complete differentiation on polyethylene terephtalate membrane inserts (surface area 0.3 cm2, pore size 0.4 µm) in 24-well format (Becton Dickinson, Pont de Claix, France). Medium was changed every two days. Differentiated cells were exposed to 10µM of DMSO, DON or D3G. The culture medium in apical side of differentiated cells in each well was replaced every two days with medium containing toxin. The TEER was measured for each well daily during 8 days using a Millicell-ERS Voltohmmeter (Millipore, Saint-Quentin-en-Yvelines, France). TEER values were expressed as $k\Omega \times cm^2$.

Immunoblotting

Caco2 cells differentiated on 24-well format (same process that for TEER), were treated with 10 µM of DMSO for control, D3G or DON for 1 hour to analyze the expression of the total and phosphorylated MAPK P38 and JNK. Proteins were extracted from cells as previously described (Pinton et al. 2009) quantified and 15 µg of total proteins was separated by SDS-PAGE. The membranes were probed with rabbit antibodies (Cell Signaling Technology, Danvers, USA) specific for: SAPK/JNK and phospho-SPAK/JNK or p38 and phospho-p38 diluted at 1:500 or GAPDH diluted at 1:1000. After washing, the membranes were incubated with 1:10,000 CF^{TM}770 goat anti-rabbit IgG (Biotium, Hayward, USA) for the detection. Antibody detection was performed using an Odyssey Infrared Imaging Scanner (Li-Cor Science Tec, les Ulis, France) with the 770nm channel. The expression of the proteins was estimated after normalization with GAPDH signal. Three independent experiments were proceeding for each cell culture condition.

Intestinal jejunal explants, preparation for microarray analysis

The microarray GPL16524 (Agilent technology, 8 x 60K) used in this experiment consisted in 43,603 spots derived from the 44K (V2:026440 design) Agilent porcine specific microarray, 9,532 genes from adipose tissue, 3,776 genes from immune system and 3,768 genes from skeletal muscle (Voillet et al. 2014). For each sample, Cyanine-3 (Cy3) labeled cRNA was prepared from 200 µg of total RNA using the One-Color Quick Amp Labeling kit (Agilent) according to the manufacturer's instructions, followed by Agencourt RNAClean XP (Agencourt Bioscience Corporation, Beverly, Massachusetts). About 600ng of Cy3-labelled cRNA was hybridized on SurePrint G3 Porcine GE microarray (8X60K) following the manufacturer's instructions. Slides were scanned immediately after washing on an Agilent G2505C Microarray Scanner with Agilent Scan Control A.8.5.1 software. All experimental details are available in the Gene Expression Omnibus (GEO) database under accession GSE66918 (http://www.ncbi.nlm.nih.gov/geo/query/acc.cgi?token=olixoosedvmdnqr &acc=GSE66918). Microarray data from Feature Extraction software was analyzed with R (www.r-project.org, R v. 3.0.1), using Bioconductor packages (www.bioconductor.org, v 2.12, ((Gentleman et al. 2004).

Statistical Analysis

For microarray data, statistical analysis was performed with R 3.0.1 software. The limma package (Ritchie et al. 2015) was used to analyze differences between treatments. A model including animal explants pairs were fitted using the limma lmFit function (Smyth 2004). A correction for multiple testing was then applied using False Discovery Rate (Benjamini and Hochberg. 1995). Probes with adjusted p-value ≤ 0.05 were considered differentially expressed between treated and control conditions. Hierarchical clustering was applied to the samples and the probes using 1-Pearson correlation coefficient as distance and Ward's criterion for agglomeration.

ESM_2 : Table of primer sequences used for RT-qPCR analysis (F: Forward; R: Reverse)

Gene symbol	Gene name	Primer sequence	References
CycloA	Cyclophilin A	F: CCCACCGTCTTCTTCGACAT	NM_214353
		R: TCTGCTGTCTTTGGAACTTTGTCT	(Curtis et al. 2009)
RPL32	Ribosomal Protein L32	F: AGTTCATCCGGCACCAGTCA	NM_001001636
		R: GAACCTTCTCCGCACCCTGT	(Pinton et al. 2010)
IL-1α	Interleukin 1- alpha	F: TCAGCCGCCCATCCA	NM_214029,1
		R: AGCCCCCGGTGCCATGT	(Cano et al. 2013)
IL-1β	Interleukin 1- beta	F: ATGCTGAAGGCTCTCCACCTC	NM_214055
		R: TTGTTGCTATCATCTCCTTGCAC	(von der Hardt et al. 2004)
IL8	Interleukin 8	F: GCTCTCTGTGAGGCTGCAGTTC	NM_213867
		R: AAGGTGTGGAATGCGTATTTATGC	(Grenier et al. 2011)
TNF-α	Tumor necrosis factor - alpha	F: ACTGCACTTCGAGGTTATCGG	NM_214022
		R: GGCGACGGGCTTATCTGA	(Meissonnier et al. 2008)
IL-17α	Interleukin 17- alpha	F: CCAGACGGCCCTCAGATTAC	AB102693
		R: CACTTGGCCTCCCAGATCAC	(Cano et al. 2013)
IL22	Interleukin 22	F: AAGCAGGTCCTGAACTTCAC	AY937228
		R: CACCCTTAATACGGCATTGG	(Cano et al. 2013)

ESM_3 : Video of DON inside the A-site of the ribosome 60S subunit
P and A sites of the ribosome 60S subunit are respectively in purple and yellow, the 3-hydroxyl group of DON is represented in red and the atom of magnesium in green, in CPK representation. Video shows a 360° view of the binding of the DON inside the A-site of the ribosome 60S subunit.
https://secure.yazibadrive.net/my/FileLink/f49e17bf-43e3-0286-d255-243243c707f9/false

ESM_4 : Video of D3G inside the A-site of the ribosome 60S subunit
P and A sites of the ribosome 60S subunit are respectively in purple and yellow, the 3-hydroxyl group of DON is represented in red and the atom of magnesium in green, in CPK representation. Video shows a 360° view of the interaction model of the D3G inside the A-site of the ribosome 60S subunit after alignment of the backbone of D3G over the DON.
https://secure.yazibadrive.net/my/FileLink/bfb9d494-c401-7764-1020-04cfc5fef3e7/false

References

- Benjamini HY and Hochberg Y (1995) Controlling the False Discovery Rate: a practical and powerful approach to multiple testing. J R Statist Soc B. 57:289-300
- Cano PM, Seeboth J, Meurens F, Cognie J, Abrami R, Oswald IP and Guzylack-Piriou L (2013) Deoxynivalenol as a new factor in the persistence of intestinal inflammatory diseases: an emerging hypothesis through possible modulation of Th17-mediated response. PLoS One 8:e53647
- Curtis MM, Way SS and Wilson CB (2009) IL-23 promotes the production of IL-17 by antigen-specific CD8 T cells in the absence of IL-12 and type-I interferons. J Immunol. 183:381-387
- Gentleman RC, Carey VJ, Bates DM, Bolstad B, Dettling M, Dudoit S, Ellis B, Gautier L, Ge Y, Gentry J, Hornik K, Hothorn T, Huber W, Iacus S, Irizarry R, Leisch F, Li C, Maechler M, Rossini AJ, Sawitzki G, Smith C, Smyth G, Tierney L, Yang JY and Zhang J. (2004) Bioconductor: open software development for computational biology and bioinformatics. Genome Biol. 5:R80
- Grenier B, Loureiro-Bracarense AP, Lucioli J, Pacheco GD, Cossalter AM, Moll WD, Schatzmayr G and Oswald IP. (2011) Individual and combined effects of subclinical doses of deoxynivalenol and fumonisins in piglets. Mol Nutr Food Res. 55:761-771

- Meissonnier GM, Pinton P, Laffitte J, Cossalter AM, Gong YY, Wild CP, Bertin G, Galtier P and Oswald IP. (2008) Immunotoxicity of aflatoxin B1: impairment of the cell-mediated response to vaccine antigen and modulation of cytokine expression. Toxicol Appl Pharmacol. 231:142-149
- Pinton P, Braicu C, Nougayrede JP, Laffitte J, Taranu I and Oswald IP (2010) Deoxynivalenol Impairs Porcine Intestinal Barrier Function and Decreases the Protein Expression of Claudin-4 through a Mitogen-Activated Protein Kinase-Dependent Mechanism. J Nutr. 140:1956-1962
- Pinton P, Nougayrède JP, Del Rio JC, Moreno C, Marin DE, Ferrier L, Bracarense AP, Kolf-Clauw M and Oswald IP. (2009) The food contaminant deoxynivalenol, decreases intestinal barrier permeability and reduces claudin expression. Toxicol Appl Pharmacol. 237:41-48
- Ritchie ME, Phipson B, Wu D, Hu Y, Law CW, Shi W and Smyth GK (2015) limma powers differential expression analyses for RNA-sequencing and microarray studies Nucleic Acids Res. 43:e47.
- Sambuy Y, De Angelis I, Ranaldi G, Scarino ML, Stammati A and Zucco F (2005) The Caco-2 cell line as a model of the intestinal barrier: influence of cell and culture-related factors on Caco-2 cell functional characteristics. Cell Biol Toxicol. 21:1-26
- Smyth GK (2004) Linear models and empirical bayes methods for assessing differential expression in microarray experiments. Stat Appl Genet Mol Biol. 3:Article3
- Voillet V, San Cristobal M, Lippi Y, Martin PG, Iannuccelli N, Lascor C, Vignoles F, Billon Y, Canario L and Liaubet L (2014) Muscle transcriptomic investigation of late fetal development identifies candidate genes for piglet maturity. BMC Genomics. 15:797
- von der Hardt K, Kandler MA, Fink L, Schoof E, Dötsch J, Brandenstein O, Bohle RM and Rascher W (2004) High frequency oscillatory ventilation suppresses inflammatory response in lung tissue and microdissected alveolar macrophages in surfactant depleted piglets. Pediatr Res. 55:339-346